LETTER TO THE EDITOR

Evanescent and real waves in quantum billiards and Gaussian beams

M V Berry

H H Wills Physics Laboratory, Tyndall Avenue, Bristol BS8 1TL, UK

Abstract. A mode in a confined planar region can contain evanescent waves in its plane-wave superposition. It would seem impossible to construct such a mode by continuation of an external scattering superposition, which must contain only real plane waves. However, evanescent waves can be expressed as the singular limit of an angular superposition of real plane waves. This is surprising because, in the direction perpendicular to that in which it decays, an evanescent wave oscillates faster than the free-space wavenumber; thus the singular superpositions lie in the class of 'superoscillatory' functions, which vary faster than any of their Fourier components. The superposition is the limit of an exact (i.e. non-paraxial and non-singular) Gaussian beam on its evanescent side slopes. Far from the axis, the beam possesses, on each side, a line of phase singularities (nodal points) which organize the global energy current. The three-dimensional generalization provides an explicit elementary construction of a superoscillatory function.

It is known that there are connections between waves confined in a domain $\mathcal{B}$ and waves scattered from the exterior of $\mathcal{B}$ (Doron and Smilansky 1992a, b, c, Blümel *et al* 1992, Dietz and Smilansky 1993). Both waves satisfy the Helmholtz equation

$$\nabla^2\psi + k^2\psi = 0 \tag{1}$$

with boundary conditions—for example Dirichlet, as we assume for simplicity in what follows. And if for some k the S-matrix has an eigenvalue unity—that is if $\mathcal{B}$ is transparent to a particular superposition of plane waves travelling in different directions and launched from outside—then that same superposition, when continued to the interior of $\mathcal{B}$, is a bound state of (1) with eigenvalue k^2.

Here I will be concerned with the reverse implication, namely that every confined mode is associated with an external superposition of plane waves for which $\mathcal{B}$ is transparent. At first this seems doubtful because of the existence of *evanescent* plane wave solutions of (1), which are inadmissible in global scattering superpositions because they grow infinitely in one direction. In two dimensions, with coordinates $r \equiv (x, y) \equiv (r, \theta)$, the plane wave solutions of (1) are

$$\psi_\alpha(r) = \exp\{ik(x\cos\alpha + y\sin\alpha)\} = \exp\{ikr\cos(\theta - \alpha)\}. \tag{2}$$

If $(-\pi \leqslant \alpha \leqslant \pi)$, this represents a real plane wave, oscillating (with wavelength $2\pi/k$) in the direction of travel α and constant along the wavefronts perpendicular to α; we call the wave real, even though the wavefunction ψ is complex, because its direction is real. If α is complex, (2) represents an evanescent plane wave oscillating,

with wavelength $2\pi/(k \cosh \operatorname{Im}\alpha)$ which is less than $2\pi/k$, along the direction $\operatorname{Re}\alpha$, and decaying exponentially in the direction $\operatorname{Re}\alpha + \pi/2 \operatorname{Sign}(\operatorname{Im}\alpha)$. The simplest example is

$$\psi_{iA}(r) = \exp\{ikx \cosh A\} \exp\{-ky \sinh A\}. \tag{3}$$

It is easy to show that evanescent waves are necessary components of some modes for some domains B, and indeed that there are modes composed entirely of evanescent waves. One way is first to specify a k, and construct an arbitrary superposition of real plane waves for which $\operatorname{Re}\psi$ has a smooth closed nodal line $\mathcal{L}$. This is a mode of (1) for the domain B whose boundary is $\mathcal{L}$; figure 1(a) shows an example. Now convert one or more of the component waves into evanescent waves, by giving their directions a small imaginary part. This perturbed superposition will have a new nodal line $\mathcal{L}$, slightly perturbed from the old one, and will be a Dirichlet mode of the B with this new $\mathcal{L}$ as boundary; figure 1(b) shows an example.
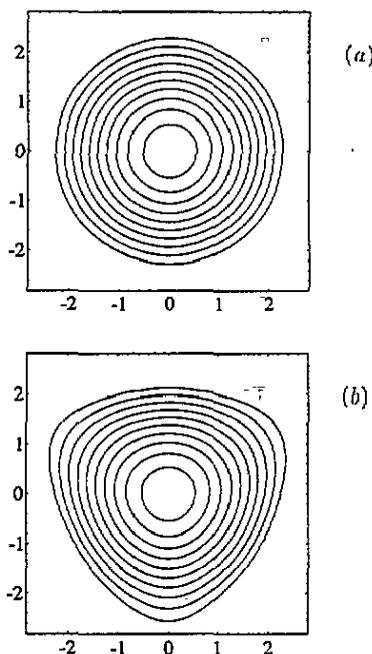

Figure 1. (a) Contours of $\operatorname{Re}\{\psi_0(r) + \psi_{2\pi/3}(r) + \psi_{-2\pi/3}(r)\}$, which is a Dirichlet mode of the domain B whose boundary—the outermost contour—is the nodal line $\mathcal{L}$ (which looks circular but in fact deviates from circularity by about 1%). (b) As (a) but for $\operatorname{Re}\{\psi_{0,1i}(r) + \psi_{2\pi/3+0.1i}(r) + \psi_{-2\pi/3+0.1i}(r)\}$; this is a mode composed entirely of evanescent waves.

I expect that, apart from some special cases such as the circle, the occurrence of evanescent waves in quantum billiard modes will be typical. Faddeev (1966) contemplated the use of growing solutions of wave equations to describe scattering, and evanescent waves have appeared in numerical computations for the B consisting of a quadrilateral with angles 90°, 90°, 45° and 135° (Richens and Berry 1981). On the other hand, a successful numerical method is based on representing ψ as a superposition containing only real plane waves (Heller 1991).

This apparent discordance between numerical methods, and also the apparent impossibility of extending modes containing evanescent waves outside $\mathcal{B}$ to become scattering superpositions, have a common origin, namely the apparent incompleteness of the set of real plane waves as a basis for representing general solutions of (1). At first thought, this incompleteness seems obvious. For example, how can the evanescent wave (3), which oscillates along x faster than the wavenumber k, be represented in terms of real plane waves, which oscillate along x at a rate which depends on direction but which never exceeds k? Surprisingly, such a representation can be constructed with arbitrary accuracy. It constitutes a two-dimensional generalization of 'superoscillatory' functions of a single variable, which oscillate over arbitrarily long ranges arbitrarily faster than any of their Fourier components. I have recently investigated the properties of these curious functions (Berry 1994) following a suggestion of Aharonov *et al* (1990).

One representation of the evanescent wave (3) as a superposition of real plane waves is

$$\psi_{iA}(r) = \lim_{\Delta \to 0} \Phi_\Delta(r) \qquad \text{where}$$

$$\Phi_\Delta(r, A) = \frac{1}{\Delta\sqrt{2\pi}} \int_{-\pi}^{\pi} d\alpha\, \psi_\alpha(r) \exp\left\{-\frac{2}{\Delta^2} \sin^2\{\tfrac{1}{2}(\alpha - iA)\}\right\}. \tag{4}$$

The intuition behind this formula is that in the limit $\Delta \to 0$ the Gaussian factor acts like a δ-function which selects the plane wave with $\alpha = iA$, which is evanescent. Of course this argument is not rigorous because iA lies outside the range of integration. Nevertheless (4) does describe an evanescent wave. This can be shown in several ways, as follows.

Substituting (2) into (4) we see that for small Δ the integral Φ_Δ is dominated by the Gaussian saddle-point at $\alpha = iA$, through which, as can easily be shown, it is possible *to deform the integration contour. The evanescent wave (3) is then obtained immediately.* I used this technique (Berry 1994) to study a variety of superoscillatory functions. The method reveals the price to be paid for superoscillations. Far from the origin, that is for $r \gg 1/\Delta^2$, the saddle moves from iA towards $\tan^{-1}(y/x)$ and Φ_Δ oscillates normally, that is with the prescribed wavelength $2\pi/\lambda$, but is exponentially large in comparison with its values near the origin where it superoscillates.

For the particular function (4) the integral can be evaluated exactly and Φ_Δ understood in more detail. Elementary transformations give

$$\Phi_\Delta(r, A) = \frac{\exp\{-1/\Delta^2\}}{\Delta\sqrt{2\pi}}$$

$$\times \int_{-\pi}^{\pi} d\alpha \, \exp\left\{\left(\frac{1}{\Delta^2}\cosh A + ikx\right)\cos\alpha + i\left(\frac{1}{\Delta^2}\sinh A + ky\right)\sin\alpha\right\}. \tag{5}$$

This can be written in terms of the modified Bessel function I_0 (Abramowitz and Stegun 1972):

$$\Phi_\Delta(r, A) = \frac{\sqrt{2\pi}\exp\{-1/\Delta^2\}}{\Delta}$$

$$\times I_0\left\{\sqrt{\left(\frac{1}{\Delta^2}\cosh A + ikx\right)^2 - \left(\frac{1}{\Delta^2}\sinh A + ky\right)^2}\right\}. \tag{6}$$

For small Δ we can use the asymptotic approximation

$$I_0(z) \approx \frac{1}{\sqrt{2\pi z}} \exp z \tag{7}$$

and show that Φ_Δ reduces to the evanescent wave (3) when $r \ll 1/\Delta^2$.

What has been shown is that the superposition (4) of real plane waves with the same k, which could be employed for example in a scattering experiment, does indeed reproduce the evanescent wave (3) in the limit $\Delta \to 0$. Therefore if the scattering space is augmented to include such singular superpositions, all modes confined in $\mathcal{B}$, including those containing evanescent waves, can be extended outside as scattering waves for which $\mathcal{B}$ is transparent. To understand the singular nature of the limit, it is convenient to relate Φ_Δ to planar analogues of the Gaussian beams of (for example) laser physics (Siegman 1986).

After defining

$$G(\xi, \eta, \rho) \equiv \sqrt{2\pi\rho} \exp(-\rho) J_0 \left\{ \sqrt{(\xi - i\rho)^2 + \eta^2} \right\} \tag{8}$$

where $J_0(z) = I_0(iz)$ is the Bessel function of the first kind, we can write

$$\Phi_\Delta(r, A) = \frac{1}{\sqrt{\cosh A}} \exp \left\{ 2 \frac{\sinh^2(A/2)}{\Delta^2} \right\} G \left\{ kx, ky + \frac{\sinh A}{\Delta^2}, \frac{\cosh A}{\Delta^2} \right\}. \tag{9}$$

The function G is that exact non-singular solution of (1) which in the paraxial approximation represents a Gaussian beam. To see this, we expand the Bessel function for large $\rho \gg \sqrt{(\xi^2 + \eta^2)}$, and obtain

$$G(\xi, \eta, \rho) \approx \frac{1}{1 + i\xi/2\rho} \exp \left\{ i\xi - \frac{\eta^2}{2(\rho + i\xi)} \right\} \tag{10}$$

which closely resembles the standard expression for a (three-dimensional) Gaussian beam (Siegman 1986), with ρ denoting the radius of the beam waist. From (9) we now arrive at the following interpretation of the plane-wave representation (4): the evanescent wave (3) is the local behaviour of a Gaussian beam G, of (large) radius $\cosh A/k\Delta^2$, on its side slopes near $(0, \sinh A/k\Delta^2)$. In the limit $\Delta \to 0$, this local behaviour extends over an infinite range of x and y.

On its evanescent side slopes, G is exponentially smaller than on its axis $\eta = 0$, since

$$G(0, \eta, \rho) \equiv \sqrt{2\pi\rho} \exp(-\rho) I_0 \left\{ \sqrt{\rho^2 - \eta^2} \right\}$$

$$\approx \left(1 - \frac{\eta^2}{\rho^2} \right)^{-1/4} \exp \left\{ \sqrt{\rho^2 - \eta^2} - \rho \right\} \qquad (\rho \gg 1, |\eta| < \rho)$$

$$\approx \exp \left\{ -\frac{\eta^2}{2\rho} \right\} \qquad (|\eta| \ll \rho). \tag{11}$$

A measure of superoscillation on these side slopes is the increase with η of the local wavenumber

$$\partial_x \operatorname{Im} \log G(0, \eta, \rho) = k \frac{\rho I_1 \left\{ \sqrt{\rho^2 - \eta^2} \right\}}{\sqrt{\rho^2 - \eta^2} I_0 \left\{ \sqrt{\rho^2 - \eta^2} \right\}}$$

$$\approx \frac{k}{\sqrt{1 - \eta^2/\rho^2}} \qquad (\eta \ll \rho)$$

$$= \tfrac{1}{2} k\rho \qquad (\eta = \rho). \tag{12}$$

The most rapid superoscillations, bigger than k by a factor $\rho/2$, therefore occur when η is close to ρ, which from (11) implies $|G| \sim \exp\{-\rho\}$.

Each evanescent wave contributing to a confined mode of β can therefore be approximated by appropriately-directed Gaussian beams aimed off-axis at $\mathcal{B}$, with impact parameter corresponding to its evanescence parameter A (equation (3)). For example, the mode shown in figure 1(b) could be approximated by three such Gaussian beams whose axes form an equilateral triangle containing $\mathcal{B}$. Better approximations need larger ρ (or smaller Δ), which implies (from (11)) that $\mathcal{B}$ lies in regions where the scattering beam is exponentially· small relative to its largest values. Therefore transparency to scattering is unlikely to be a sensitive means of detecting modes containing evanescent waves.
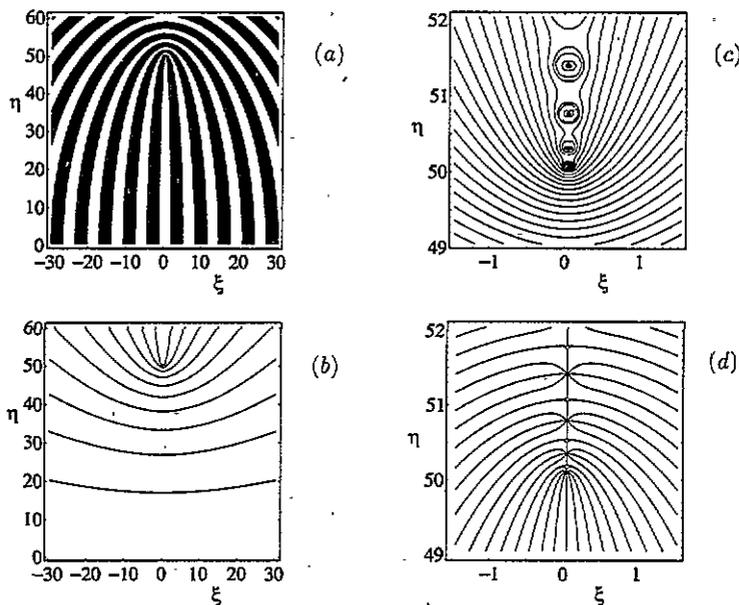

Figure 2. Gaussian beam $G(\xi, \eta, \rho)$ (equation (8)) for $\rho = 50$. (a) Nodal domains of Re G (white positive, black negative). (b) Contours of $\log_{10} |G|$ (increasing upwards). To the accuracy of the picture, these contours are also flow lines of the current Im $G^* \nabla G$. (c) Magnification of (b), showing zeros of $|G|$ (black dots), which are also vortices of current and phase dislocations. (d) Phase contours (wavefronts) of G, at intervals of $\pi/2$, showing wavefront dislocations where all phases meet, and, between them, phase saddles.

Pictures of the exact Gaussian beam (8) are instructive. Figure 2(a) shows the nodal line of Re G for $\rho = 50$. For small ξ they crowd close together as η increases, provided $|\eta|$ is less than the beam radius ρ. This crowding indicates that G superoscillates in this region. (It is amusing to note that these nodal lines are closed when the picture is reflected in the ξ axis and so could represent the boundaries $\mathcal{L}$ of a set of domains $\mathcal{B}$ within which Re G is a confined mode.) Figure 2(b) shows the contours of $|G|$, whose exponential decay away from the beam axis $\eta = 0$ indicates local evanescence.

If this picture is magnified (figure 2(c)), small dark spots become visible on the η axis for $|\eta| > \rho$. These are zeros of the complex function G, that is wavefront dislocations (Nye and Berry 1974, Berry 1981) where the phase χ of G is singular (figure 2(d)). Although they lie in a region where the beam intensity is numerically insignificant ($|G| = O \exp(-\rho)$), they

play an important role in the global organization of the energy current. For reasons explained in the appendix, the current lines coincide approximately with the intensity contours in figures 2(*b*) and 2(*c*). Current flows from negative to positive ξ, with an η component whose sign is signξ signη except near the segments $|\eta| > \rho$ of the η axis. There, the interference of the counterflowing currents (up and down the η axis), generates vortices circulating about the dislocation points (see Hirschfelder *et al* 1974a, b, Hirschfelder and Tang 1976a, b, for examples of wave vortices in quantum mechanics). The dislocations close to $\eta = \rho$ provide dramatic illustrations of superoscillations, because they are topological structures separated by scales much smaller (by a factor of order $1/\rho$) than the wavelength of the waves in the beam. As η increases, so does the dislocation spacing, which gradually approaches π.

It is also instructive to explore the evanescent-wave and superoscillation aspects of the more familiar three-dimensional Gaussian beams. For a beam travelling in the ξ direction, with perpendicular coordinates η and ζ, the counterpart of (8) is

$$G_3(\xi, \eta, \zeta, \rho) \equiv 2\rho \exp(-\rho) \frac{\sin\left\{\sqrt{(\xi - i\rho)^2 + \eta^2 + \zeta^2}\right\}}{\sqrt{(\xi - i\rho)^2 + \eta^2 + \zeta^2}}. \tag{13}$$

Expansion near the axis gives (10) with η^2 replaced by $\eta^2 + \zeta^2$ and without the factor 2 in the denominator. The wave that is evanescent on the side slopes—the counterpart of (9)—is

$$\Phi_{3,\Delta}(r, A) = \frac{1}{\cosh A} \exp\left\{2\frac{\sinh^2(A/2)}{\Delta^2}\right\} G_3\left\{kx, ky + \frac{\sinh A}{\Delta^2}, kz + \frac{\sinh A}{\Delta^2}, \frac{\cosh A}{\Delta^2}\right\} \tag{14}$$

(where now $r = (x, y, z)$). Near the x axis and with $|kx| \ll \cosh A/\Delta^2$, this is an evanescent plane wave travelling in the x direction and decaying along the positive y and z directions:

$$\Phi_{3,\Delta}(r, A) \to \exp\{ikx \cosh A\} \exp\left\{-k(y + z) \sinh A/\sqrt{2}\right\}. \tag{15}$$

Like their two-dimensional counterparts, the waves (13) and (14) are superpositions of real plane waves whose wavevectors have the same length. For example, (13) can be written as

$$G_3(\xi, \eta, \zeta, \rho) = \frac{1}{2\pi} \rho \exp(-\rho) \iint_{\text{unit sphere}} d^2\Omega \exp\{i\Omega \cdot (\xi - i\rho, \eta, \zeta)\} \tag{16}$$

where Ω denotes a unit vector in three dimensions. A similar formula enables (14) to be expressed as a superposition of real plane waves with wavenumber k. On the x axis this can be written (after evaluating one of the angular integrals) as

$$\Phi_{3,\Delta}((x, 0, 0), A) = \frac{2\exp\left\{-\frac{1}{\Delta^2}\right\} \sin\left\{\sqrt{\left(kx - i\frac{\cosh A}{\Delta^2}\right)^2 + \frac{\sinh^2 A}{\Delta^2}}\right\}}{\sqrt{\left(kx - i\frac{\cosh A}{\Delta^2}\right)^2 + \frac{\sinh^2 A}{\Delta^2}}}$$

$$= \frac{\exp\left\{-\frac{1}{\Delta^2}\right\}}{k\Delta^2} \int_{-k}^{k} dq \exp\{iqx\} \left[\exp\left\{+q\frac{\cosh A}{k\Delta^2}\right\} J_0\left\{\sqrt{k^2 - q^2}\right\} \frac{\sinh A}{k\Delta^2}\right] \tag{17}$$

which is a superposition of Fourier components band-limited by $\pm k$ (it corresponds to the representation (4) with $q = k \cos \alpha$). It is a superoscillatory function of x, as is shown by the following limiting forms (easily checked by computation):

$$\Phi_{3,\Delta}((x,0,0), A) \approx \exp\{ikx \cosh A\} \qquad \left(kx \ll \frac{\cosh A}{\Delta^2}\right)$$

$$\approx \exp\{ikx\} \frac{\exp\left\{\dfrac{2\sinh^2\{A/2\}}{\Delta^2}\right\}}{i\Delta^2 kx} \qquad \left\{kx \gg \frac{\cosh A}{\Delta^2}\right\}. \tag{18}$$

This is interesting because it exemplifies a superoscillatory function composed entirely of elementary functions, a possibility not envisaged by Berry (1994).

A final remark concerns the standard theory of non-paraxial Gaussian beams. In this theory (see, e.g., Siegman 1986), the formulae (8) and (13) are written with J_0 replaced by the outgoing Bessel function $H_0^{(1)}(\ldots)$ and its three-dimensional counterpart $\sin(\ldots)/\ldots$ replaced by the outgoing wave $\exp\{i \ldots\}/\ldots$). It is then noted, following Deschamps (1971) (see also Felsen 1976), that these correspond to waves emerging from a complex source on the ξ axis at $\xi = i\rho$,. However, although in the paraxial regime these waves reduce to (10) and its three-dimensional analogue, they possesses singularities at the real points $(0, \pm\rho)$ and on the real circle ($\xi = 0, \eta^2 + \zeta^2 = \rho^2$), whence branch cuts issue to infinity. Therefore they are inappropriate as representations of freely-propagating beams. Related to this is another property which makes the $H_0^{(1)}$ and $\exp\{i \ldots\}/\ldots$ waves unsuitable for our present purpose: they consist of superpositions involving complex directions, and therefore evanescent waves. The representations (8) and (13) avoid these disadvantages.

I thank Professor Uzy Smilansky for conversations which led to this work.

Appendix. Current lines and intensity contours

The energy current is $\operatorname{Im} G^* \nabla G$, which is parallel to $\nabla \chi$. To the accuracy of figures 2(b) and 2(c), the current lines are identical to the contours of the intensity $|G|$. This is not obvious. In most of the r plane, this is except for the immediate neighbourhood of the ξ axis and the segments $|\eta| > \rho$ of the η axis, the smallness ($O(1/\rho)$) of the angle between the two sets of lines follows from the 'single-wave' approximation (7), in which the exponential dominates. It is a consequence of the orthogonality of the real and imaginary parts of the gradient of the complex distance $\sqrt{[(\xi - i\rho)^2 + \eta^2]}$, and this in turn follows from the complexified Hamilton–Jacobi equation.

Near $|\eta| > \rho$ on the η axis, (7) breaks down because its single exponential must be supplemented by $i \exp\{+z\}$ (this quantity is negligible elsewhere). In this region too the lines of $\nabla \chi$ and the contours of $|G|$ are very similar, because they are locked together by two sets of coincident singularities. First are the current vortices (phase dislocations) and zeros of $|G|$, generated by the interference of the two waves. These sets of points coincide (at zeros of $J_0\{\sqrt{(\eta^2 - \rho^2)}\}$). Second are the stagnation points of current (phase saddles) and the saddles of $|G|$, which lie between the dislocations. These sets of points also coincide (at zeros of $J_1\{\sqrt{(\eta^2 - \rho^2)}\}$). A calculation shows that the angle between the intensity contours and the current lines is α, where

$$\sin \alpha = \frac{\nabla|G| \cdot \nabla \chi}{|\nabla|G|||\nabla\chi|} = \frac{2\operatorname{Re} f \operatorname{Im} f}{\sqrt{(|f|^2 t \cdot t^*)^2 - (\operatorname{Re} f^2)^2}} \tag{A1}$$

in which f and the complex unit vector t are defined by

$$f \equiv J_0\left\{\sqrt{(\xi + i\rho)^2 + \eta^2}\right\} J_1\left\{\sqrt{(\xi - i\rho)^2 + \eta^2}\right\}$$

$$t \equiv \nabla\sqrt{|(\xi - i\rho)^2 + \eta^2|} = \frac{(\xi - i\rho, \eta)}{\sqrt{|(\xi - i\rho)^2 + \eta^2|}}. \tag{A2}$$

Numerical evaluation shows that $\alpha < 3°$ (and is generally very much smaller) for the contours shown in figures 2(b) and 2(c).

The $\nabla\chi$ lines and the $|G|$ contours are, however, discordant (i.e. α is large) in a very narrow strip enclosing the ξ axis, where the intensity contours and current lines are perpendicular (these lines are not shown in figure 2(b)).

References

Abramowitz M and Stegun I A 1972 *Handbook of Mathematical Functions* (Washington, DC: National Bureau of Standards)
Aharonov Y, Anandan J, Popescu S and Vaidman L 1990 *Phys. Rev. Lett.* **64** 2965–8
Berry M V 1981 Singularities in waves *Les Houches Lecture Series Session XXXV* ed R Balian, M Kléman and J-P Poirier (Amsterdam: North-Holland) pp 453–543
Berry M V 1994 Faster than Fourier *Fundamental Problems in Quantum Theory* ed J A Anandan and J Safko (Singapore: World Scientific) to appear
Blümel R, Dietz B, Jung C and Smilansky U 1992 *J. Phys. A: Math. Gen.* **25** 1483–502
Deschamps G A 1971 *Electronics Lett.* **7** 684–5
Dietz B and Smilansky U 1993 *Chaos* **3** 581–9
Doron E and Smilansky U 1992a *Phys. Rev. Lett.* **68** 1255–8
—— 1992b *Chaos* **2** 117–24
—— 1992c *Nonlinearity* **5** 1055–84
Faddev L D 1966 *Sov. Phys. Dokl.* **10** 1033–5
Felsen L B 1976 *J. Opt. Soc. Am.* **66** 751–60
Heller E J 1991 Wavepacket dynamics and quantum chaology *Les Houches Lecture Series Session LII* ed M-J Giannoni, A Voros and J Zinn-Justin (Amsterdam: Elsevier) pp 547–663
Hirschfelder J O, Christoph A C and Palke W E 1974a *J. Chem. Phys.* **61** 5435–55
Hirschfelder J O, Goebel C J and Bruch L W 1974b *J. Chem. Phys.* **61** 5456–9
Hirschfelder J O and Tang K T 1976a *J. Chem. Phys.* **64** 760–85
—— 1976b *J. Chem. Phys.* **65** 470–86
Nye J F and Berry M V 1974 *Proc. R. Soc.* A **336** 165–90
Richens P J and Berry M V 1981 *Physica* **1D** 495–512
Siegman A E 1986 *Lasers* (Mill Valley: University Science Books)